Journal of Applied Mechanics and Technical Physics, Vol. 43, No. 1, pp. 76–82, 2002

RELAMINARIZATION OF A TURBULENT BOUNDARY LAYER WITH A MACH NUMBER $M_\infty = 4$

M. A. Goldfeld, R. V. Nestoulia, and A. N. Shiplyuk

UDC 532.526

Results of experimental studies are presented on relaminarization of a supersonic turbulent boundary layer behind an expansion fan for a free-stream Mach number $M_\infty = 4$ *within a range of Reynolds numbers* $Re_1 = 8 \cdot 10^6$–$26 \cdot 10^6$ m^{-1}. *Experimental data on distributions of the mean velocity and mass-flow fluctuations and the skin friction force are obtained. Partial relaminarization of the boundary layer is reached in the experiments. The calculations of relaminarization criteria show that they can be used to predict the onset of the relaminarization process at high supersonic flow velocities.*

Introduction. It is currently of interest to study the behavior of a supersonic turbulent boundary layer in flows with high favorable and adverse pressure gradients caused by shock or expansion waves. Interaction of a turbulent boundary layer with a distributed or local adverse pressure gradient has been well studied, whereas the action of a favorable pressure gradient on a turbulent boundary layer has not been adequately examined. One of the features of the action of a strong favorable pressure gradient on a turbulent boundary layer is the possibility of reverse transition of the boundary layer from the turbulent state to the laminar one (relaminarization) [1–4]. This means a decrease in heat fluxes and skin friction, which is particularly important for supersonic and hypersonic flow velocities [5, 6]. In addition, experimental data on the relaminarization process may be used in constructing turbulence models for such flows [7].

As was shown in [3–7], the basic governing parameters of the relaminarization process are the longitudinal pressure gradient, Reynolds and Mach numbers, and skin friction upstream of the region where the pressure gradient acts on the boundary layer. The effect of these parameters on relaminarization was studied most comprehensively for subsonic flow velocities [2, 4, 8]. In particular, Warnack and Fernholz [4] studied the effect of the longitudinal pressure gradient and Reynolds number on relaminarization, reached complete relaminarization of the turbulent boundary layer, performed detailed measurements of velocity profiles, skin friction force, and fluctuating characteristics, and analyzed their spectral composition in the region of relaminarization. Detailed studies of relaminarization of a turbulent boundary layer for high subsonic and supersonic flow velocities are much more seldom [9–12]. Thus, only heat fluxes were measured in studying relaminarization arising in the flow around turbine blades and in supersonic nozzles [5, 6]. Velocity profiles and integral parameters of the boundary layer for free-stream Mach numbers $M_\infty = 2$–4 were measured only in [9, 10]. The results of [9] were obtained in a blowdown wind tunnel with a high initial level of turbulence in a narrow range of Reynolds numbers, which seems to be the reason for partial relaminarization and a small length of the relaminarized flow region. At the same time, it was found that the boundary layer remained kinematically nonequilibrium at a length up to 200 boundary-layer thicknesses, which agrees with the data of [4] for subsonic flows.

None of the works dealing with relaminarization of a supersonic turbulent boundary layer reports direct measurements of the skin friction force. The questions of the possibility of complete relaminarization of a turbulent boundary layer at supersonic and hypersonic flow velocities and the dependence of this process on the longitudinal pressure gradient and Reynolds number remain also open. All investigations of relaminarization at supersonic velocities were performed in commonly used wind tunnels with a rather high level of free-stream fluctuations, which could also hinder the development of the relaminarization process.

Institute of Theoretical and Applied Mechanics, Siberian Division, Russian Academy of Sciences, Novosibirsk 630090. Translated from Prikladnaya Mekhanika i Tekhnicheskaya Fizika, Vol. 43, No. 1, pp. 91–99, January–February, 2002. Original article submitted April 23, 2001, revision submitted August 22, 2001.

 0021-8944/02/4301-0076 $27.00

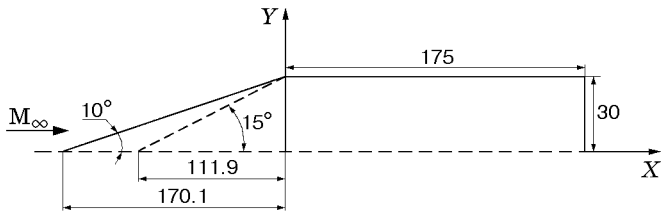

Fig. 1. Schematic of the cone–cylinder model.

TABLE 1

$\mathrm{Re}_1 \cdot 10^{-6}$, m^{-1}	δ_0, mm	$\mathrm{Re}^{**} \cdot 10^{-6}$, m^{-1}	$-(d\bar{P}/dX) \cdot 10^{-6}$, m^{-1}
		$\theta = 10°$	
19.3	—	—	0.47
16.5	—	—	0.39
13.6	1.45	0.93	0.33
		$\theta = 15°$	
24.6	0.69	1.06	1.09
21.5	0.72	0.86	0.88
16.8	0.83	0.67	0.70

Systematic studies of relaminarization, especially at high supersonic velocities, are of much interest both for science and applications.

The present work has the following objectives: to verify the possibility of obtaining complete relaminarization of a supersonic turbulent boundary layer, to study the influence of the favorable pressure gradient and Reynolds number on relaminarization, to measure the skin friction force by the optical method, and to study the profiles of mass-flow fluctuations during relaminarization of a supersonic boundary layer.

1. Model and Experimental Technique. The necessary condition for the beginning of relaminarization is the action of a strong favorable pressure gradient on a turbulent boundary layer. To obtain the favorable pressure gradient in experiments, we used an expansion flow arising in the flow around a corner configuration of an axisymmetric cone–cylinder model (Fig. 1). The gas-dynamic parameters of this flow are close to the Prandtl–Meyer flow. The use of replaceable cones with apex half-angles $\theta = 10$ and 15° allowed us, changing the longitudinal pressure gradient, to determine its effect on the relaminarization process.

The experiments were performed in a T-325 low-turbulent supersonic wind tunnel of the Institute of Theoretical and Applied Mechanics of the Siberian Division of the Russian Academy of Sciences for a free-stream Mach number $\mathrm{M}_\infty = 4$ within the range of Reynolds numbers $\mathrm{Re}_1 = (8 \cdot 10^6)$–$(26 \cdot 10^6)$ m^{-1}. The parameters measured in the experiments were the static pressure and the wall temperature on the conical and cylindrical parts of the model, the Pitot pressure distributions behind the first shock wave upstream of the probe (the Pitot tube thickness was 0.18 mm), the mass-flow fluctuations over the boundary-layer height, and the skin friction force [13]. The accuracy of model mounting in terms of the angles of attack and sideslip was checked both by direct measurements before the experiments and by the static pressure distribution on the conical and cylindrical parts of the model at points located along a circumference. The velocity profiles in the boundary layer were calculated by the measurement results for total pressure profiles under the assumption that the static pressure across the boundary layer was constant. The boundary-layer thickness was determined by the coordinate with $U = 0.99U_e$, where U_e is the flow velocity at the boundary-layer edge. A dimensionless longitudinal coordinate X/δ_0 (δ_0 is the boundary-layer thickness on the conical part of the model) was used to analyze experimental data. The values of δ_0 for various Reynolds numbers are listed in Table 1. The temperature distribution in the boundary layer was calculated using the modified Crocco integral. The mass-flow fluctuations were measured by a constant-current hot-wire anemometer.

Preliminary theoretical estimates showed that the length of the cone generatrix is insufficient for the formation of a natural turbulent boundary layer for low Reynolds numbers [14]. Therefore, a 0.4 mm annular sand turbulizer was mounted on the conical part of the model. The distance between the turbulizer and the corner point of the contour was greater than 120 boundary-layer thicknesses.

The state of boundary-layer relaminarization was determined by the boundary-layer profile, skin friction measurement results and integral characteristics of the boundary layer and mass-flow fluctuations. The velocity

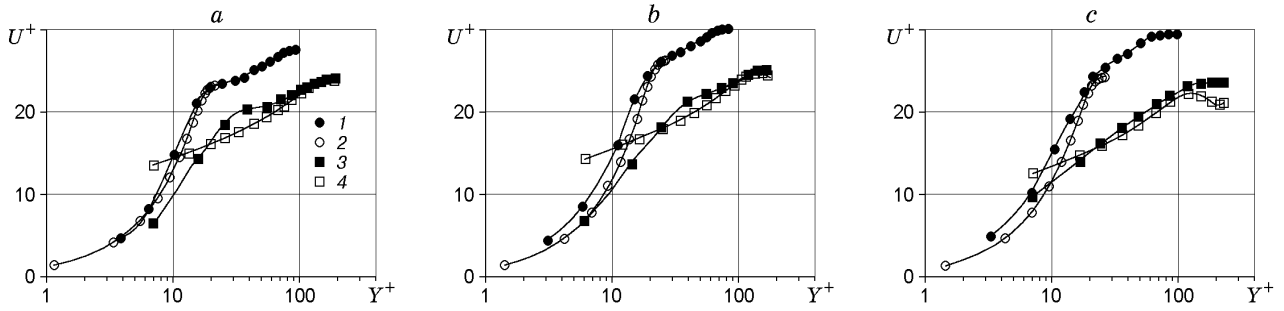

Fig. 2. Mean velocity profiles in the boundary layer on the cylindrical part of the model ($\theta = 15^\circ$) for $X/\delta_0 = 12$ (a), 44 (b), and 64 (c); curve 1 refers to $\mathrm{Re}_1 = 16 \cdot 10^6$ m^{-1}, curve 2 is the Blasius profile for curve 1, curve 3 refers to $\mathrm{Re}_1 = 26 \cdot 10^6$ m^{-1}, and curve 4 is the wall-wake law for curve 3.

profiles were analyzed within the framework of the wall-wake law [15]. The plot of the universal logarithmic law of velocity distributions $U^+(Y^+)$ (U^+ and Y^+ are the dimensionless velocity and coordinate that enter the wall-wake law) in a turbulent boundary layer has a linear section, which drastically decreases because of partial relaminarization of the boundary layer. After complete relaminarization, the linear section disappears, and the velocity profile should be described by the Blasius law. Boundary-layer relaminarization can be also estimated by the boundary-layer shape factor H_{12} transformed for an incompressible flow; its value was determined as the ratio of the boundary-layer displacement and momentum thicknesses transformed for an incompressible flow: $H_{12} = \delta^*/\delta^{**}$. The parameters of the incompressible flow were calculated using the Dorodnitsyn–Stewartson transformation [15]. Their values are $H_{12} \approx 1.5$ and $H_{12} \approx 2.25$–2.55 for the turbulent and laminar boundary layer, respectively.

Skin friction was determined by the oil-film optical method [13]. In addition, the skin friction force was found from the measured velocity profiles [10]. Obviously, the significant decrease in shear stress in the laminar flow regime in the boundary layer and its characteristic change in the laminar–turbulent transition can be used as the most reliable method of detection of boundary-layer relaminarization.

2. Discussion of Results. To determine the characteristics of the boundary layer on the conical part of the model, we found the minimum free-stream Reynolds numbers at which a turbulent boundary layer is formed. The flow character in the boundary layer on the conical part of the model was determined by the results of Schlieren pictures and measurements of velocity profiles and mass-flow fluctuations. An analysis of the results obtained shows that the turbulent boundary layer is formed beginning from the minimum Reynolds numbers $\mathrm{Re}_1 = 13.6 \cdot 10^6$ m^{-1} for $\theta = 10^\circ$ and $\mathrm{Re}_1 = 16.8 \cdot 10^6$ m^{-1} for $\theta = 15^\circ$. The corresponding values of the Reynolds number Re^{**} based on the momentum thickness are listed in Table 1. The turbulent boundary layer may also exist for Reynolds numbers lower than these values, but in this case, the influence of artificial turbulization on the relaminarization process is possible.

Based on the static pressure measurements along the model generatrix, we obtained the longitudinal pressure gradient. Table 1 gives the values of $d\bar{P}/dX$ in the region $0 < X/\delta_0 < 7$ immediately behind the corner point of the model contour ($\bar{P}$ is the static pressure normalized to the free-stream static pressure). A drastic decrease in pressure gradient down to values close to zero is observed downstream of this region. It follows from Table 1 that the longitudinal pressure gradient in experiments with $\theta = 15^\circ$ almost twice as large as for $\theta = 10^\circ$ for identical Reynolds numbers. With increasing Re_1, the longitudinal pressure gradient increases, which seems to be related to the change in the ratio of displacement thicknesses on the conical and cylindrical parts of the model for different Reynolds numbers.

In analyzing the velocity profiles on the conical part of the model for apex half-angles $\theta = 10$ and 15°, it was found that a developed turbulent boundary layer is formed upstream of the corner point of the model contour, which is well described within the framework of the wall-wake law. Partial relaminarization of the boundary layer is observed on the cylindrical part of the model behind the corner point of the model contour (Fig. 2). It follows from Fig. 2 that partial relaminarization of the boundary layer is manifested in the fact that the near-wall part of the boundary layer is well described by the theoretical Blasius profile. At the same time, the external part of the boundary layer has no clear logarithmic section, but there is a wake component typical of a turbulent boundary layer. The thickness of the laminarized part of the boundary layer for $X/\delta_0 = 12$ is approximately 0.25δ (δ is the local boundary-layer thickness), which is significantly greater than the values typical of the laminar sublayer

TABLE 2

$\mathrm{Re}_1 \cdot 10^{-6}$, m^{-1}	H_{12}				
	$X/\delta_0 = 12$	$X/\delta_0 = 20$	$X/\delta_0 = 30.6$	$X/\delta_0 = 44$	$X/\delta_0 = 64$
16.8	1.91	1.98	2.03	2.06	2.03
21.5	1.73	1.88	1.98	1.96	1.83
26.4	1.67	1.80	1.84	1.74	1.66

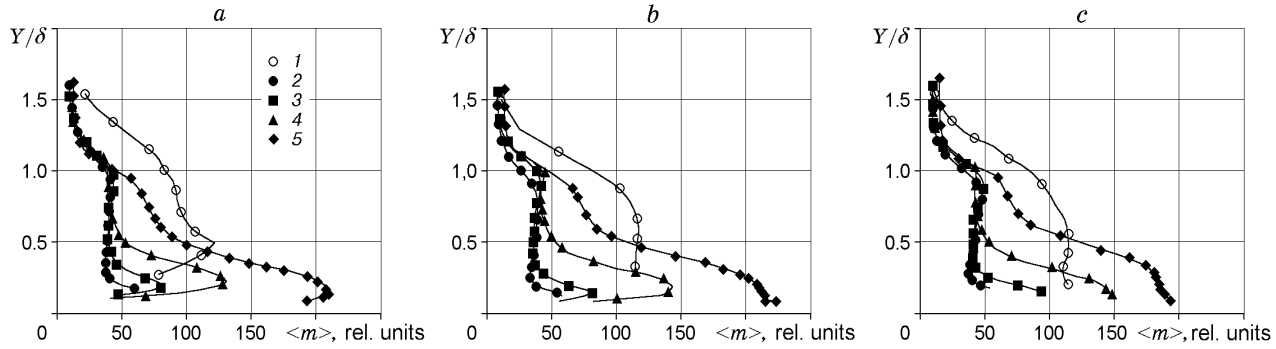

Fig. 3. Profiles of mass-flow fluctuations in the boundary layer for $\mathrm{Re}_1 = 16 \cdot 10^6$ (a), $21 \cdot 10^6$ (b), and $26 \cdot 10^6$ m^{-1} (c) and $X/\delta_0 = -17.3$ (1), 12 (2), 20 (3), 44 (4), and 64 (5).

of the turbulent boundary layer. The velocity in the laminarized part of the profile is 90% of the velocity at the boundary-layer edge. For low Reynolds numbers, the thickness of the laminarized part of the velocity profile increases downstream of the corner point, and the near-wall laminarized part of the boundary layer becomes more filled, which is evidenced by the deviation of experimental data from the theoretical laminar Blasius profile. The thickness of the laminarized part of the boundary layer increases downstream from 0.25δ for $X/\delta_0 = 12$ to 0.4δ for $X/\delta_0 = 44$. An increase in the Reynolds number leads to an increase in the fullness of the near-wall laminarized part of the boundary layer downstream of the corner point, and the boundary layer is turbulent already for $X/\delta_0 = 64$. The special feature of velocity profiles for $\theta = 10^\circ$ is that the thickness of the relaminarized part of the boundary layer decreases. The reason is that the value of the favorable pressure gradient in this case is twice as small as for the flow-deflection angle $\theta = 15^\circ$. An analysis of boundary-layer velocity profiles shows that the length of the relaxation region (reverse transition to a turbulent flow) is different and depends substantially on the Reynolds number. Within the length examined (up to $130\delta_0$), the reverse transition to a turbulent flow occurred only for $\mathrm{Re}_1 = 26 \cdot 10^6$ m^{-1}.

Based on the measurement results for velocity profiles, the integral characteristics of the boundary layer were calculated, including its transformed (for a constant-density flow) parameters. It was found that the transformed shape factor of the boundary layer H_{12} on the cylindrical part of the model depends on the Reynolds number and changes downstream (Table 2). Behind the corner point of the model contour, the shape factor H_{12} increases with decreasing Re_1 and tends to values typical of a laminar boundary layer. An insignificant increase in the shape factor is observed downstream of the corner point of the model contour, which indicates intensification of the relaminarization process. With increasing Re_1, beginning from a certain distance, the value of the transformed shape factor tends again to the value $H_{12} = 1.66$ typical of a turbulent boundary layer.

The profile of mass-flow fluctuations in the relaminarization region has also a complex two-layer character. A comparison of data in Fig. 3 shows that the change in mass-flow fluctuations is significantly different in the boundary layer upstream and downstream of the expansion fan. The quantity $\langle m \rangle$ in Fig. 3 is proportional to the relative root-mean-square fluctuations of the mass flow. Upstream of the corner point of the model contour, for all Reynolds numbers, the profiles of the mass-flow fluctuations correspond to a developed turbulent boundary layer [10]. The action of a strong favorable pressure gradient leads to a significant decrease (by a factor of 2 to 3) in the level of mass-flow fluctuations directly behind the corner point of the contour. The special feature of the profile of mass-flow fluctuations on the cylindrical part of the model in the relaminarization region is that it has two levels of fluctuations: at the upper edge of the boundary layer and in the near-wall region. Mass-flow fluctuations at the boundary-layer edge increase insignificantly downstream, and their level depends weakly on the Reynolds number. In the near-wall part of the boundary layer, immediately behind the corner point of the model contour, there appears

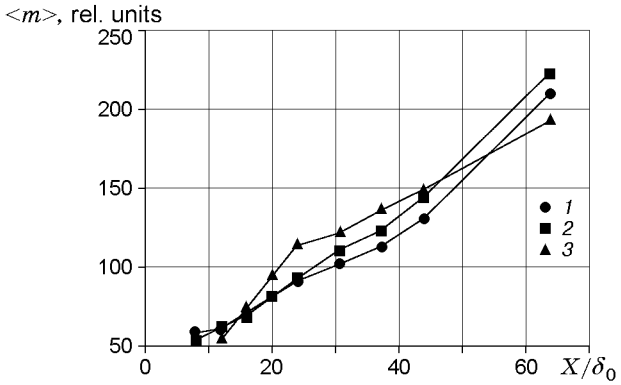

Fig. 4. Near-wall maximum of mass-flow fluctuations versus the coordinate for $\mathrm{Re}_1 = 16 \cdot 10^6$ (points 1), $21 \cdot 10^6$ (points 2), and $26 \cdot 10^6$ m^{-1} (points 3).

a peak of mass-flow fluctuations, which rapidly increases downstream. Goldfeld et al. [10] also obtained a two-peak distribution of mass-flow fluctuations with a near-wall maximum of fluctuations ($Y_{\max}/\delta \approx 0$), but boundary-layer relaminarization was not observed. In the present work, the maximum value of mass-flow fluctuations is reached at a certain distance from the surface (about 0.2δ), and then the near-wall peak of fluctuations increases downstream. The maximum level of fluctuations for $X/\delta_0 = 64$ is greater than the level of fluctuations in the turbulent boundary layer on the cone. Further downstream, the near-wall peak of fluctuations moves toward the boundary-layer edge, and the width of its base for $X/\delta_0 = 44$ is approximately equal to 50% of the boundary-layer thickness.

The dependence of the near-wall peak of mass-flow fluctuations on the longitudinal coordinate for various Reynolds numbers is shown in Fig. 4. For $X/\delta_0 < 13$, the values of $\langle m \rangle$ decrease with increasing Reynolds number. This indicates that an increase in the longitudinal pressure gradient (see Table 1) suppresses mass-flow fluctuations in the near-wall part of the boundary layer. This behavior of mass-flow fluctuations is typical only of the region where the longitudinal pressure gradient is other than zero. For $X/\delta_0 > 13$ (in the region where the longitudinal pressure gradient is almost absent), the growth rate of the near-wall maximum of fluctuations increases with increasing free-stream Reynolds number. The growth of the near-wall peak of fluctuations indicates the beginning of the laminar–turbulent transition in the near-wall laminarized part of the boundary layer.

The distribution of the skin friction force τ_w was obtained by the oil-film method. Figure 5 shows that a strong decrease in skin friction is observed behind the corner point of the model contour, which indicates that the flow character in the boundary layer changes. The greatest decrease in skin friction occurs immediately behind the corner point. For $\mathrm{Re}_1 = 16 \cdot 10^6$ m^{-1} and $X/\delta_0 > 50$, the value of τ_w is approximately constant and lower than in the flow region with a pressure gradient. This distribution of skin friction indicates intensification of the relaminarization process downstream of the corner point for this Reynolds number, which is in agreement with the data obtained by analysis of velocity profiles and transformed shape factor of the boundary layer (see Table 2). An increase in Re_1 leads to an increase in the skin friction force for $X/\delta_0 > 50$, and a skin friction distribution typical of the laminar–turbulent transition is observed for $\mathrm{Re}_1 = 26 \cdot 10^6$ m^{-1}. It follows from here than the development of the process of reverse transition of the relaminarized boundary layer into the turbulent state depends strongly on the Reynolds number.

Figure 5 shows also the calculation results for the skin friction force obtained by the integral Kutateladze–Leont'ev method for a turbulent boundary layer and for skin friction calculated using the experimental velocity profiles. The Kutateladze–Leont'ev calculations were performed using the longitudinal distribution of static pressure obtained in experiments. For different Reynolds numbers, there are qualitative and quantitative differences in skin friction distributions obtained by the oil-film technique and calculated by the Kutateladze–Leont'ev method. This difference shows that the boundary layer on the cylindrical part of the model is kinematically nonequilibrium.

The experimental data obtained allowed us to check the applicability of the existing criteria for high supersonic velocities. The values of the gradient-free criterion were determined by the formula [11] $\Lambda = C_p/C_f \geqslant 60$–$75$, where C_p is the pressure coefficient calculated by the difference in pressures on the conical and cylindrical parts of the model and C_f is the skin friction coefficient on the conical part of the model ahead of the corner point. It was found in calculations that $\Lambda = 55.4$, 52.5, and 60.9 for $\mathrm{Re}_1 = 16 \cdot 10^6$, $21 \cdot 10^6$, and $26 \cdot 10^6$ m^{-1}, respectively,

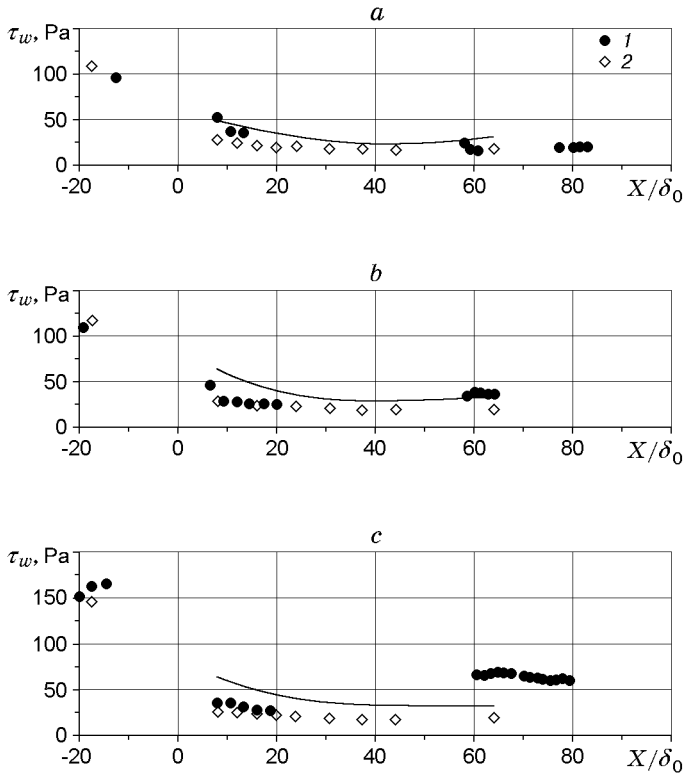

Fig. 5. Skin friction distribution along the model for $\mathrm{Re}_1 = 16 \cdot 10^6$ (a), $21 \cdot 10^6$ (b), and $26 \cdot 10^6$ m^{-1} (c); points 1 refers to the measurement results obtained by the oil-film method and points 2 refers to the calculation based on the measured velocity profiles; the solid curve is the calculation by the Kutateladze–Leont'ev method.

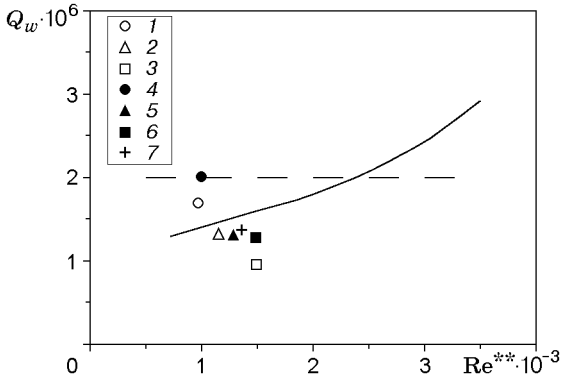

Fig. 6. Relaminarization criterion versus Re^{**}: the solid and dashed curves refer to the experimental data of [6] and [1], respectively; points 1–3 refer to $\mathrm{Re}_1 = 16 \cdot 10^6$, $21 \cdot 10^6$, and $26 \cdot 10^6$ m^{-1}, respectively, and $\theta = 15^\circ$ and $X/\delta_0 = 4$, points 4–6 refer to $\mathrm{Re}_1 = 16 \cdot 10^6$, $21 \cdot 10^6$, and $26 \cdot 10^6$ m^{-1}, respectively, and $\theta = 15^\circ$ and $X/\delta_0 = 8$, and points 7 refer to $\mathrm{Re}_1 = 13 \cdot 10^6$ m^{-1}, $\theta = 10^\circ$, and $X/\delta_0 = 8$.

and $\theta = 15^\circ$ and $\Lambda = 18.6$ for $\mathrm{Re}_1 = 13.6 \cdot 10^6$ m^{-1} and $\theta = 10^\circ$. The value of the relaminarization criterion for the model with $\theta = 15^\circ$ for all Reynolds numbers is close to the lower boundary of the relaminarization region $\Lambda \geqslant 60$–75, whereas for the model with $\theta = 10^\circ$, relaminarization of the turbulent boundary layer is impossible. The relaminarization criterion $Q_w(\mathrm{Re}^{**}) = \mu_w(dU/dX)/(\rho_e U_e^2)$ [6] was also calculated; it takes into account the longitudinal pressure gradient. Figure 6 shows the relaminarization criterion as a function of Re^{**}. It follows from Fig. 6 that the flow parameters obtained in experiments correspond to the value of the relaminarization criterion for which partial or complete relaminarization of the turbulent boundary layer is obtained, depending on the pressure gradient and Reynolds number. The use of the gradient relaminarization criterion allows one to predict the onset

of relaminarization more accurately. The results of comparison of the above values of Λ and the data in Fig. 6 show that they are contradictory. According to the data of Narasimha and Vishwanath [11], relaminarization is impossible for the flow-deflection angle $\theta = 15°$, and even more so for $\theta = 10°$, whereas the use of the gradient criterion of relaminarization allows one to predict the onset of relaminarization and partial relaminarization.

Conclusions. The boundary-layer study performed at high supersonic velocities within the Reynolds number range $\mathrm{Re}_1 = 13 \cdot 10^6$–$26 \cdot 10^6$ allows us to draw the following conclusions:

— Partial relaminarization of the boundary layer is possible at high Mach numbers; in this case, the near-wall part of the boundary layer (up to 0.4δ) is laminar;

— The Reynolds number affects mainly the length of the relaminarized flow region, which decreases with increasing Reynolds number;

— With increasing longitudinal pressure gradient in the region of its interaction with the boundary layer, the mass-flow fluctuations in the near-wall part of the boundary layer decrease;

— Partial relaminarization of a turbulent boundary layer is accompanied by the appearance of a peak of mass-flow fluctuations in the near-wall laminarized part of the boundary layer; the value of this peak increases downstream;

— The existing criteria of relaminarization predict the onset of relaminarization at high supersonic velocities rather accurately.

REFERENCES

1. B. E. Launder, "Laminarization of the turbulent boundary layer in a severe acceleration," *Trans. ASME*, **34**, Part 2, 707–709 (1964).
2. V. C. Patel and M. R. Head, "Reversion of turbulent to laminar flow," *J. Fluid Mech.*, **34**, 371–392 (1968).
3. M. A. Badri-Narayan and V. Ramjee, "Criteria for reverse transition in a two-dimensional boundary layer flow," *J. Fluid Mech.*, **35**, 225–241 (1969).
4. D. Warnack and H. H. Fernholz, "The effect of a favorable pressure gradient and of the Reynolds number on an incompressible axisymmetric turbulent boundary layer. Part 2. The boundary layer with relaminarization," *J. Fluid Mech.*, **359**, 351–381 (1998).
5. M. E. Deich and L. Ya. Lazarev, "Transition of a turbulent boundary layer into a laminar state," *Inzh.-Fiz. Zh.*, **7**, No. 4, 18–24 (1964).
6. J. L. Nash-Webber and G. C. Oates, "An engineering approach to the design of laminarizing flows," *J. Basic Trans. ASME*, No. 4, 897–904 (1972).
7. B. Aupoix and S. Viala, "Prediction of boundary layer relaminarization using low Reynolds number turbulence models," AIAA Paper No. 95-0862 (1995).
8. R. Narasimha and K. R. Sreenivasan, "Relaminarization in highly accelerated turbulent boundary layers," *J. Fluid Mech.*, **61**, 417–473 (1973).
9. M. A. Goldfeld, "On reverse transition of compressible turbulent boundary layer in a transverse flow around a convex corner configuration," in: *Proc. of the Laminar–Turbulent Transition Symposium* (Novosibirsk, July 13–19, 1984), Springer-Verlag, Berlin (1985), pp. 515–520.
10. M. A. Goldfeld, V. N. Zinov'ev, and V. A. Lebiga, "Structure and fluctuating characteristics of a compressible turbulent boundary layer behind an expansion fan," *Izv. Akad. Nauk SSSR, Mekh. Zhidk. Gaza*, No. 1, 21–29 (1987).
11. R. Narasimha and P. R. Vishwanath, "Reverse transition at an expansion corner in supersonic flow," *AIAA J.*, **13**, No. 5, 693–695 (1975).
12. J. P. Dussauge and J. Gaviglio, "The rapid expansion of a supersonic turbulent flow: role of bulk dilatation," *J. Fluid Mech.*, **174**, 81–112 (1987).
13. R. V. Nestoulia, S. B. Nikiforov, and A. A. Pavlov, "Development of the oil film method of skin friction measurement for curved and arbitrary oriented surfaces," in: *Proc. of the Int. Conf. on the Methods of Aerophysical Research* (Novosibirsk, June 28–July 3, 1998), Part 1, Publication of the Siberian Division of the Russian Academy of Sciences Publ., Novosibirsk (1998), pp. 167–172.
14. A. A. Maslov and S. G. Shevel'kov, "Features of laminar–turbulent transition of the boundary layer on a cone," *Izv. Akad. Nauk SSSR, Mekh. Zhidk. Gaza*, No. 6, 23–27 (1985).
15. G. Schlichting, *Boundary Layer Theory*, McGraw-Hill, New York (1968).